Supplementary materials

Model name	SSP5-8.5	SSP3-7.0	SSP2-4.5
ACCESS-CM2	3	3	3
ACCESS-ESM1-5	10	10	30
AWI-CM-1-1-MR	1	5	1
BCC-CSM2-MR	1	1	1
CAS-ESM2-0	1	1	1
CESM2	4	100	3
CESM2-WACCM	3	3	3
CIESM	0	0	1
CMCC-CM2-SR5	1	1	1
CMCC-ESM2	1	1	1
CanESM5	50	50	50
CanESM5-CanOE	3	3	3
E3SM-1-1	1	0	0
EC-Earth3	52	52	64
EC-Earth3-AerChem	0	2	0
EC-Earth3-CC	1	0	1
EC-Earth3-Veg	5	3	5
EC-Earth3-Veg-LR	3	3	3
FGOALS-f3-L	1	1	1
FIO-ESM-2-0	3	0	3
GFDL-CM4	1	0	1
GFDL-ESM4	1	1	3
GISS-E2-1-G	7	15	19
GISS-E2-1-H	0	0	5
HadGEM3-GC31-LL	0	0	1
INM-CM4-8	1	1	1
INM-CM5-0	1	5	1
IPSL-CM5A2-INCA	0	1	0
IPSL-CM6A-LR	7	11	11
KACE-1-0-G	3	3	3
MIROC-ES2L	1	5	24
MIROC6	50	3	22
MPI-ESM1-2-LR	10	10	10
MRI-ESM2-0	2	5	4
NESM3	0	0	2
NorESM2-LM	1	1	2
NorESM2-MM	1	1	1
TaiESM1	1	1	1
UKESM1-0-LL	0	12	13
Total	231	314	299

Table S1 Summary of CMIP6 simulations considered in this study. For each model, the number of available ensemble members is reported for the SSP2-4.5, SSP3-7.0, and SSP5-8.5 scenarios. Totals across models are provided in the last row.

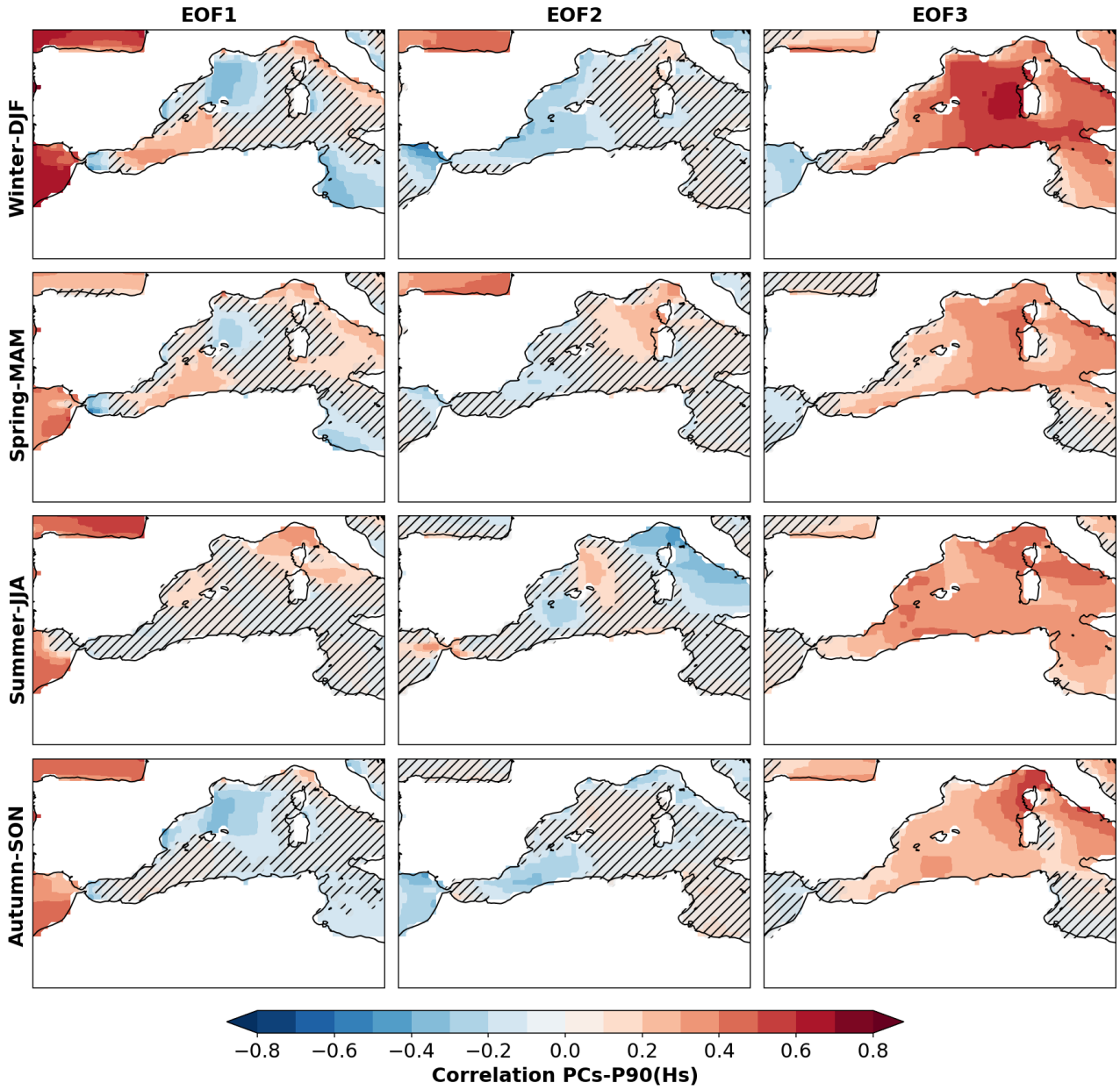

Figure S1. Spatial correlation between the first three principal components (PC1-PC3) of sea-level pressure EOFs and extreme significant wave height (Hs), defined using the daily 90th percentile, for each season. Black-hatched areas indicate regions where correlations are not statistically significant ($p \geq 0.05$). The green marker highlights the location of maximum correlation for PC3 in winter (DJF), located near Corsica. The color scale reflects both the magnitude and sign of the correlation.

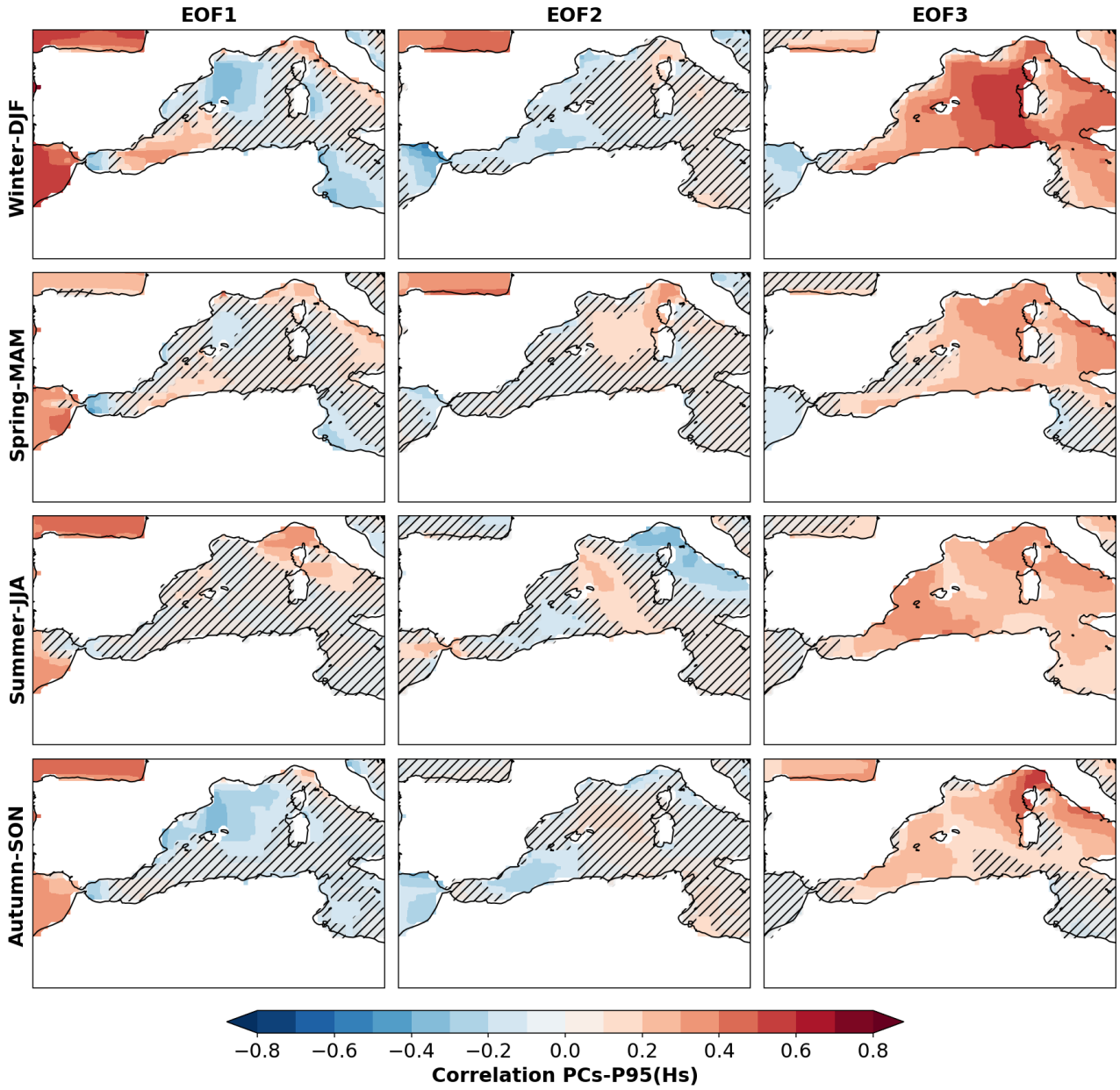

Figure S2. Spatial correlation between the first three principal components (PC1-PC3) of sea-level pressure EOFs and extreme significant wave height (Hs), defined using the daily 95th percentile, for each season. Black-hatched areas indicate regions where correlations are not statistically significant ($p \geq 0.05$). The green marker highlights the location of maximum correlation for PC3 in winter (DJF), located near Corsica. The color scale reflects both the magnitude and sign of the correlation.

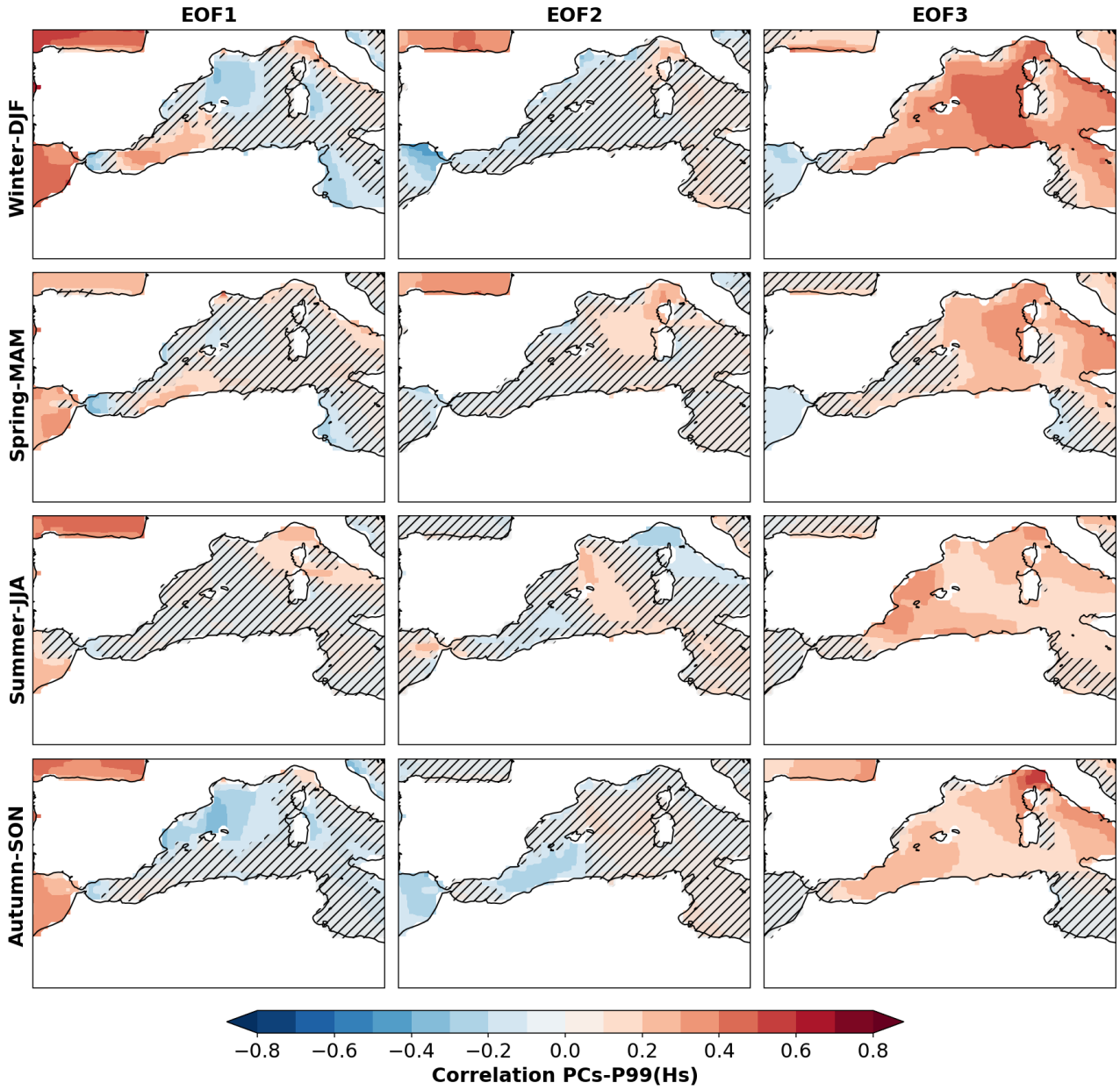

Figure S3. Spatial correlation between the first three principal components (PC1-PC3) of sea-level pressure EOFs and extreme significant wave height (Hs), defined using the daily 99th percentile, for each season. Black-hatched areas indicate regions where correlations are not statistically significant ($p \geq 0.05$). The green marker highlights the location of maximum correlation for PC3 in winter (DJF), located near Corsica. The color scale reflects both the magnitude and sign of the correlation.

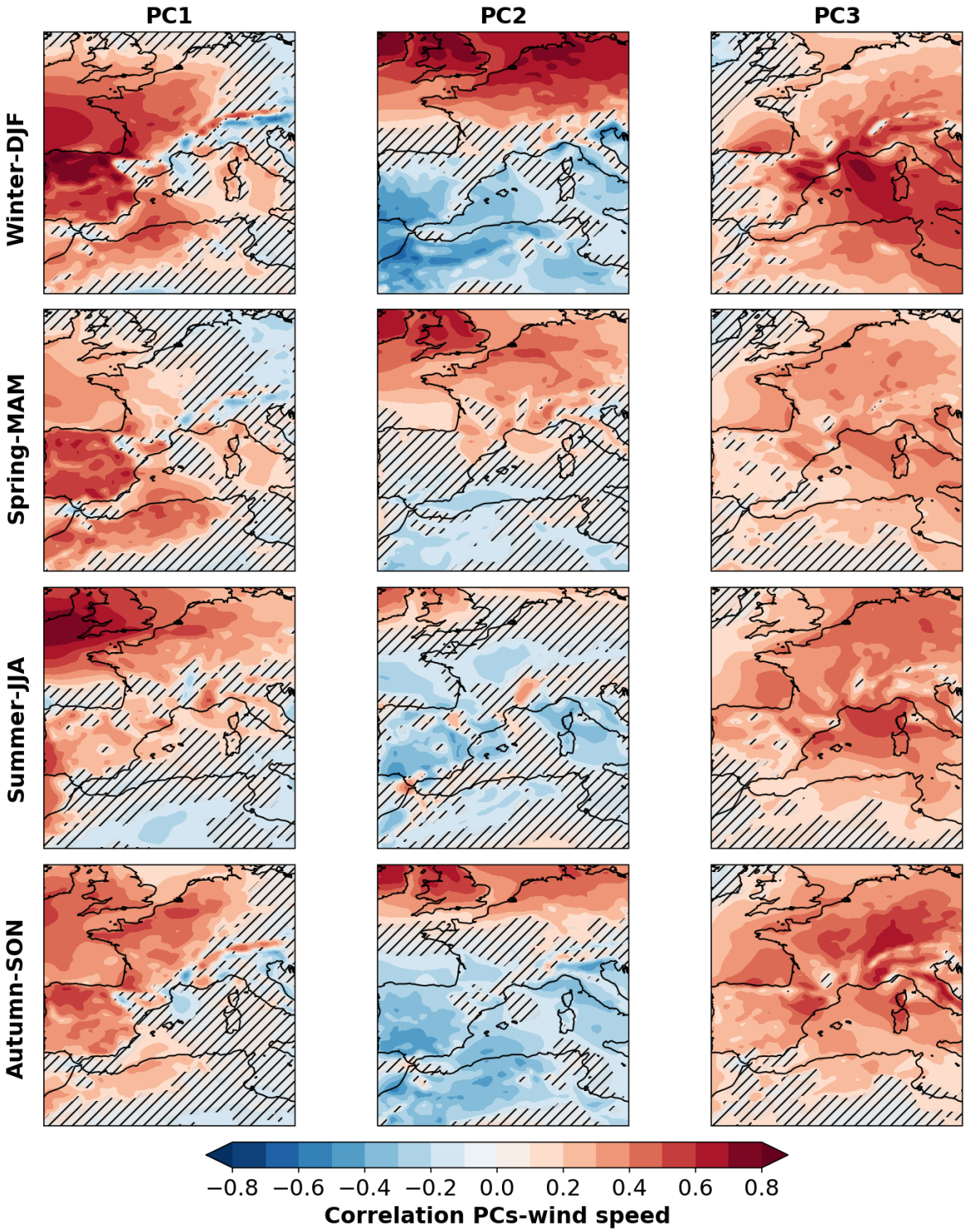

28

29 **Figure S4** Spatial correlation between the first three principal components (PC1, PC2, PC3) of SLP
30 EOFs and 10 m wind speed for each season. Grey-hatched regions denote non-significant correlations
31 ($p \geq 0.05$). The green marker indicates the location of maximum local correlation for PC3 in winter.
32 The color scale represents correlation strength and sign.

33

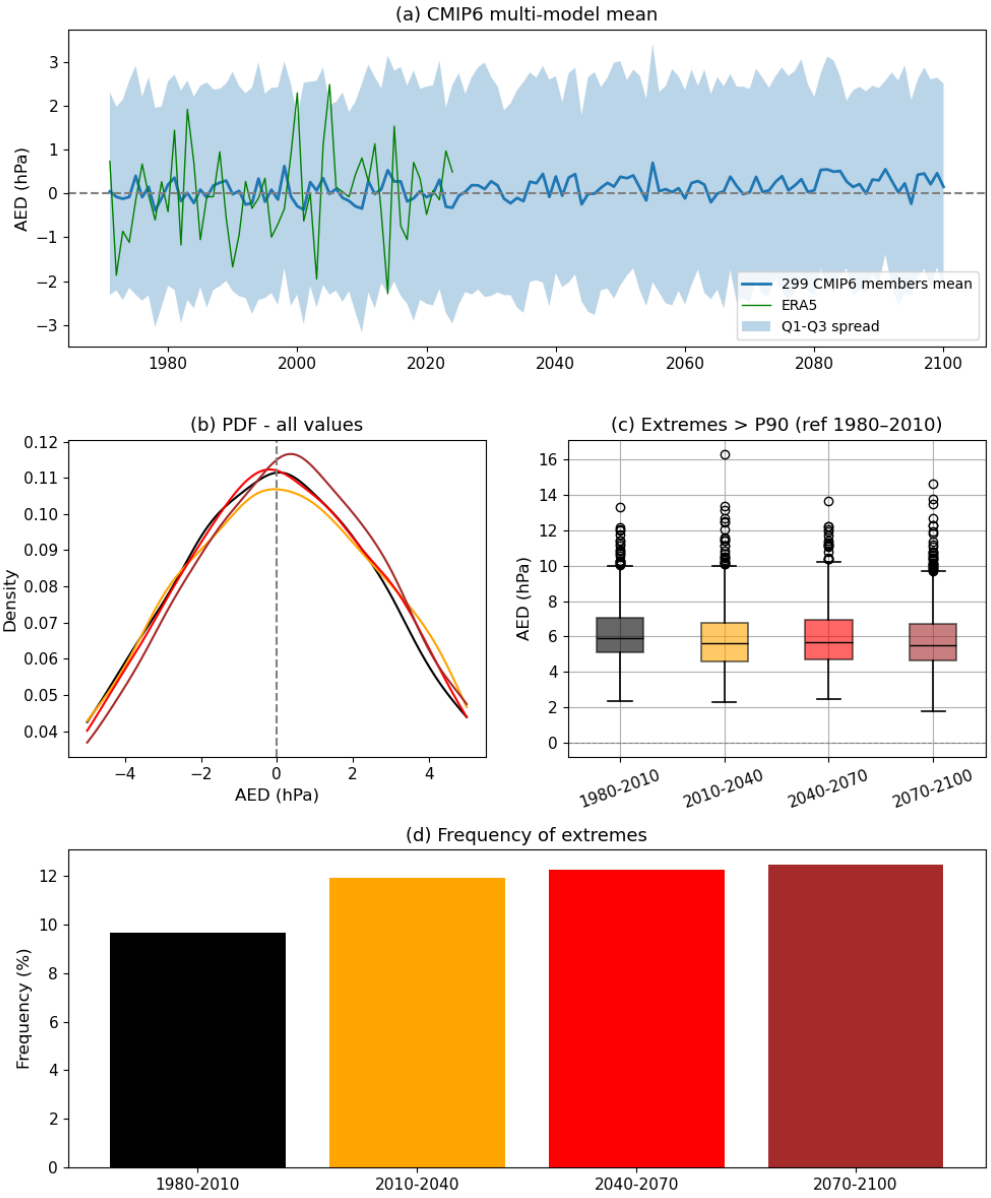

Figure S5 Projected changes in the AED in CMIP6 simulations under the SSP2-4.5 scenario. (a) Multi-model mean evolution of the AED index computed from sea-level pressure differences between the northeastern Atlantic and central Europe. The blue line represents the ensemble mean across 231 CMIP6 members, while the shaded envelope indicates the interquartile spread among models. The index is expressed relative to the 1970-2010 baseline. (b) Probability density functions (PDFs) of AED values for four time periods (1980-2010, 2010-2040, 2040-2070, and 2070-2100), illustrating changes in the distribution of the circulation index. (c) Distribution of extreme AED events exceeding the 90th percentile threshold defined from the 1980-2010 reference period. Boxplots show the median, interquartile range, and outliers across all model members. (d) Frequency of extreme AED events relative to the reference period. Results indicate a progressive increase in the occurrence of strong positive dipole phases during the twenty-first century.

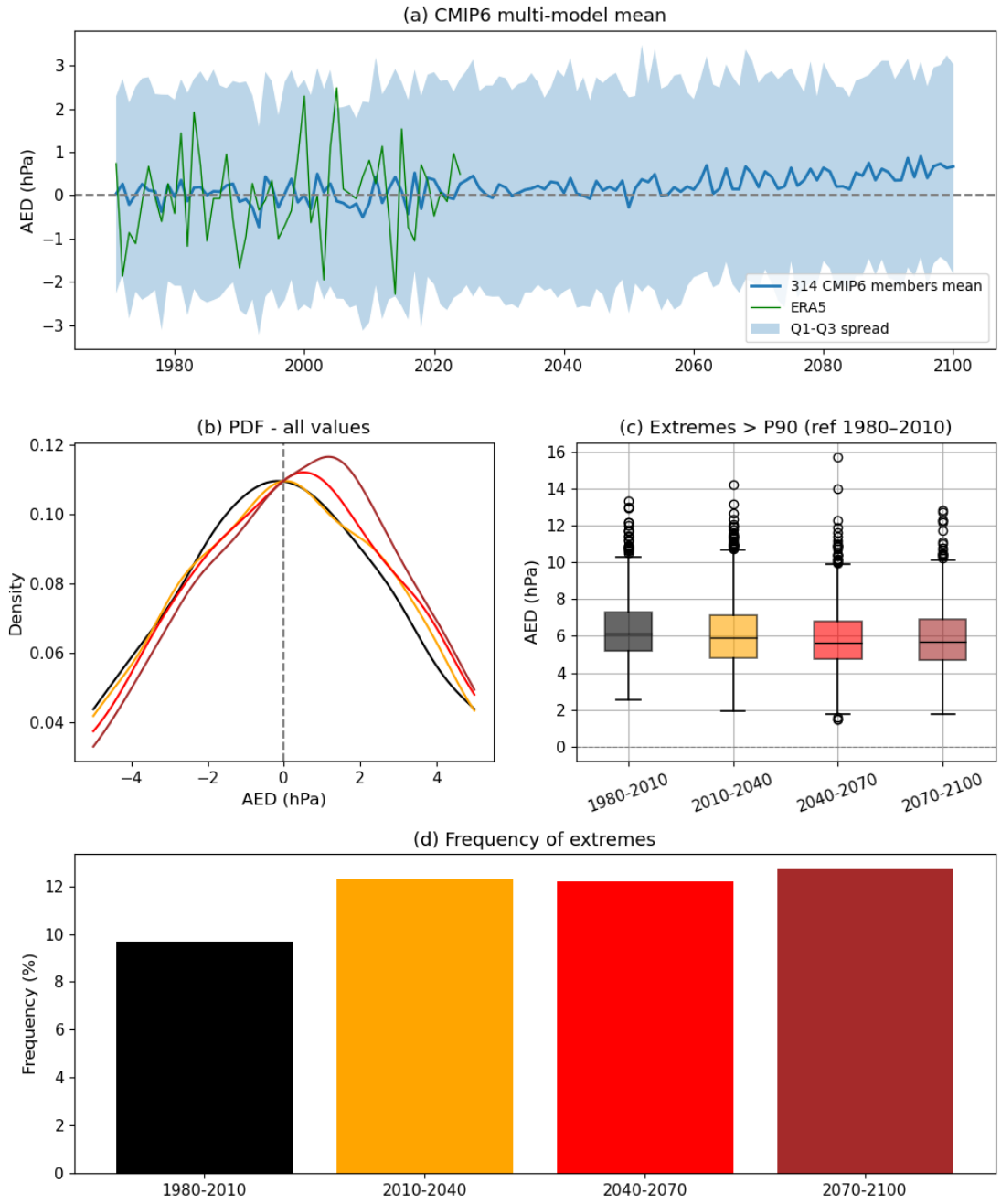

Figure S6 Projected changes in the AED in CMIP6 simulations under the SSP3-7.0 scenario. (a) Multi-model mean evolution of the AED index computed from sea-level pressure differences between the northeastern Atlantic and central Europe. The blue line represents the ensemble mean across 231 CMIP6 members, while the shaded envelope indicates the interquartile spread among models. The index is expressed relative to the 1970-2010 baseline. (b) Probability density functions (PDFs) of AED values for four time periods (1980-2010, 2010-2040, 2040-2070, and 2070-2100), illustrating changes in the distribution of the circulation index. (c) Distribution of extreme AED events exceeding the 90th percentile threshold defined from the 1980-2010 reference period. Boxplots show the median, interquartile range, and outliers across all model members. (d) Frequency of extreme AED events relative to the reference period. Results indicate a progressive increase in the occurrence of strong positive dipole phases during the twenty-first century.